Cell Reports Medicine, Volume *2*

Supplemental information

Hypoxia-sensing CAR T cells provide safety and efficacy in treating solid tumors

Paris Kosti, James W. Opzoomer, Karen I. Larios-Martinez, Rhonda Henley-Smith, Cheryl L. Scudamore, Mary Okesola, Mustafa Y.M. Taher, David M. Davies, Tamara Muliaditan, Daniel Larcombe-Young, Natalie Woodman, Cheryl E. Gillett, Selvam Thavaraj, John Maher, and James N. Arnold

Supplemental Information

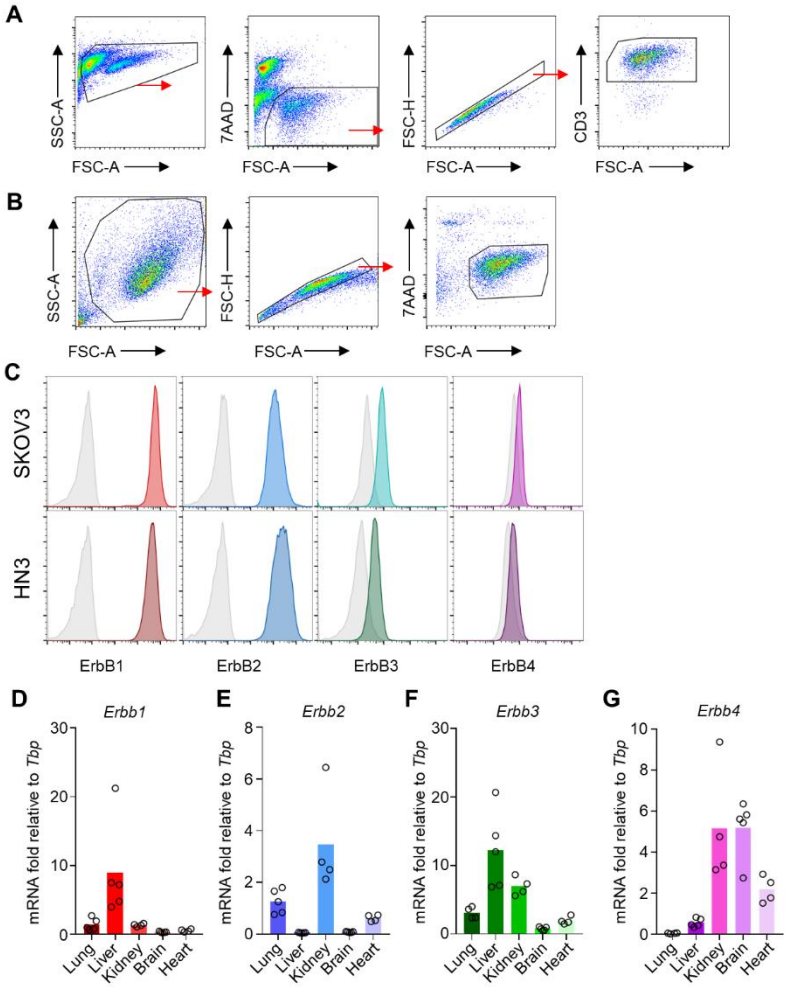

Figure S1. Flow cytometry gating strategies and ErbB receptor expression in cell lines and healthy tissues. Related to Figures 1-4. (**A, B**) Example of the flow cytometry gating strategy for live ($7AAD^-$), singlet, $CD3^+$ T-cells (**A**) and tumor cell lines (**B**). (**C**) Live gated tumor cell (SKOV3 and HN3) surface expression of ErbB1-4 (colored histograms) against their respective isotype control staining (grey histograms). (**D**-**G**) mRNA expression of *Erbb1* (**D**), *Erbb2* (**E**), *Erbb3* (**F**), *Erbb4* (**G**) genes relative to the housekeeping gene *Tbp* in the indicated tissues (n = 6). All experiments are representative of a biological repeat. Bar charts show the group mean and each point represents each individual mouse.

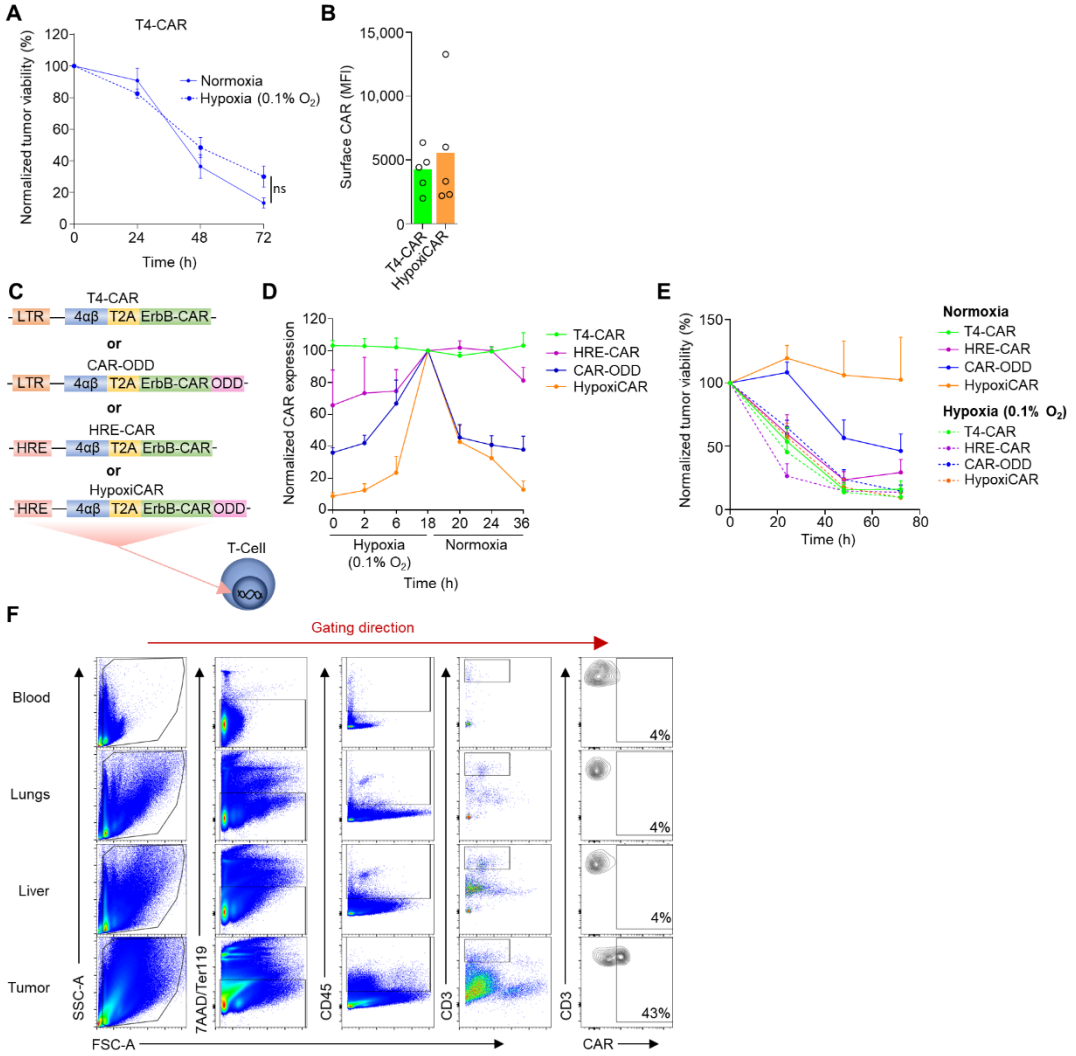

Figure S2. HypoxiCAR's dual oxygen-sensing modules synergize to provide superior stringency in sensing hypoxia. Related to Figures 2 and 3. (**A**) *In vitro* SKOV3 tumor cell killing by human T4-CAR T-cells (CAR^+ effector T-cell to target tumor cell ratio 1:1) in normoxic and hypoxic conditions (0.1% O_2) (n=4). (**B**) HypoxiCAR and T4-CAR T-cells exposed to 18h hypoxic (0.1% O_2) conditions were assessed for relative surface CAR expression/cell presented as median fluorescence intensity of staining/cell (MFI) using flow cytometry analyses (n=5). (**C-E**) Schematic diagram depicting the constructs, and their modular arrangements, which were stably transduced into human T-cells (**C**). Surface CAR expression on T4-CAR, HRE-CAR, CAR-ODD and HypoxiCAR human T-cells at the indicated times under hypoxia (0.1% O_2) or normoxia assessed using flow cytometry analyses, values normalized to 18h hypoxia (n=4) (**D**). *In vitro* SKOV3 tumor cell killing by T4-CAR, HRE-CAR, CAR-ODD and HypoxiCAR human T-cells (CAR^+ effector T-cell to target tumor cell ratio 4:1) in normoxic and hypoxic conditions (0.1% O_2) (**E**). (**F**) Representative flow cytometry dot/contour plots for the gating strategy from enzyme-dispersed tumors and healthy tissues alongside the blood from mice which had been injected both i.v. and i.t. with $7.5x10^5$ and $2.5x10^5$ of human HypoxiCAR T-cells, respectively, 72 h prior to sacrifice. Stained for live cells ($7AAD^-$, $Ter119^-$), $CD45^+$ $CD3^+$ T-cells and their surface CAR expression. Positive gates were applied based on isotype staining. All experiments are representative of a biological repeat. For line graphs, dots mark the mean and error bars the s.e.m.

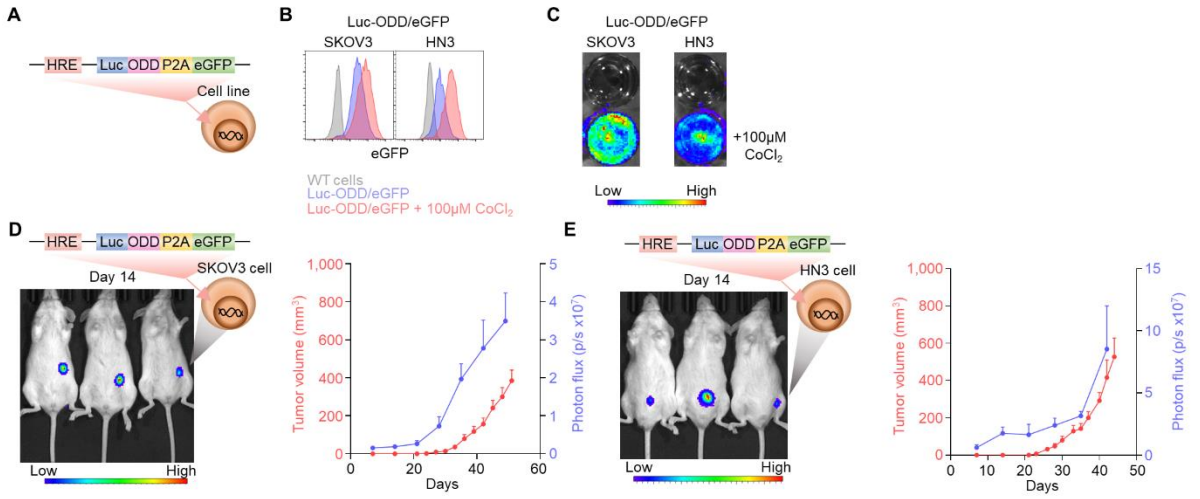

Figure S3. Hypoxia is a characteristic of even early tumor microenvironments. Related to Figure 4. (**A**) Schematic diagram depicting the 'dual-sensing' hypoxia reporter construct, and its modular arrangements, which were stably transduced into SKOV3 and HN3 tumor cells. (**B**) Representative flow cytometry histograms, gating on live ($7AAD^-$) cells, from the hypoxia reporter (Hypoxi-Luc transduced) cell lines. eGFP can be observed under conditions of normoxia in these cells, as in the absence of an ODD, the HRE module alone results in leaky expression (Figure S2C-E). (**C**) Assessing luciferase activity in Hypoxi-Luc transduced tumor cell lines in the presence or absence of 100μM $CoCl_2$, to mimic hypoxia-mediated HIF1α stabilization. (**D, E**) Representative bioluminescence images of 3 representative mice at day 14 post inoculation with hypoxia reporter SKOV3 (**D**) and HN3 (**E**) cell lines (left of each panel) and the tumor volume (red line, y-axis left) plotted against the bioluminescence signal (blue line, y-axis right) across n=6 mice for each respective tumor cell line (right panel). All experiments are representative of a biological repeat. For line graphs, dots mark the mean and error bars the s.e.m.

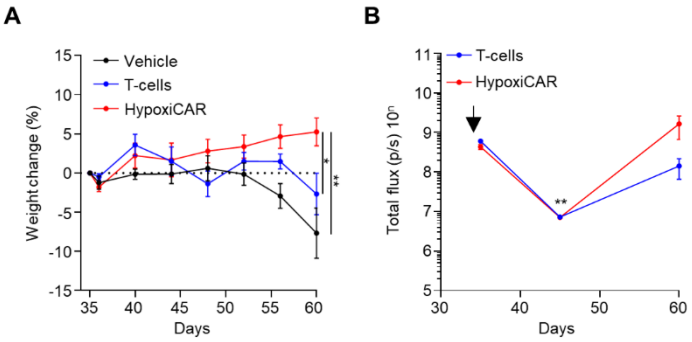

Figure S4. HypoxiCAR T-cell toxicity and persistence in mice. Related to Figure 4. Thirty two days post subcutaneous injection of SKOV3 tumor cells, when tumors were palpable, mice were infused i.v. with either vehicle (n=6) or $10x10^6$ luciferase reporter HypoxiCAR (n=7) or control reporter T-cells (n=7) (schematic for experiment shown in Figure 4G). (**A**) Weight change of the mice post infusion. (**B**). Bioluminescence imaging was performed on the whole body of mice to track the prevalence of the infused HypoxiCAR T-cells on the indicated days. Arrow marks the point of HypoxiCAR T-cell infusion. Data presented as photons/second (p/s). Experiments is representative of a biological repeat. Line charts, the dots mark the mean and error bars s.e.m. .* $P<0.05$,** $P<0.01$.

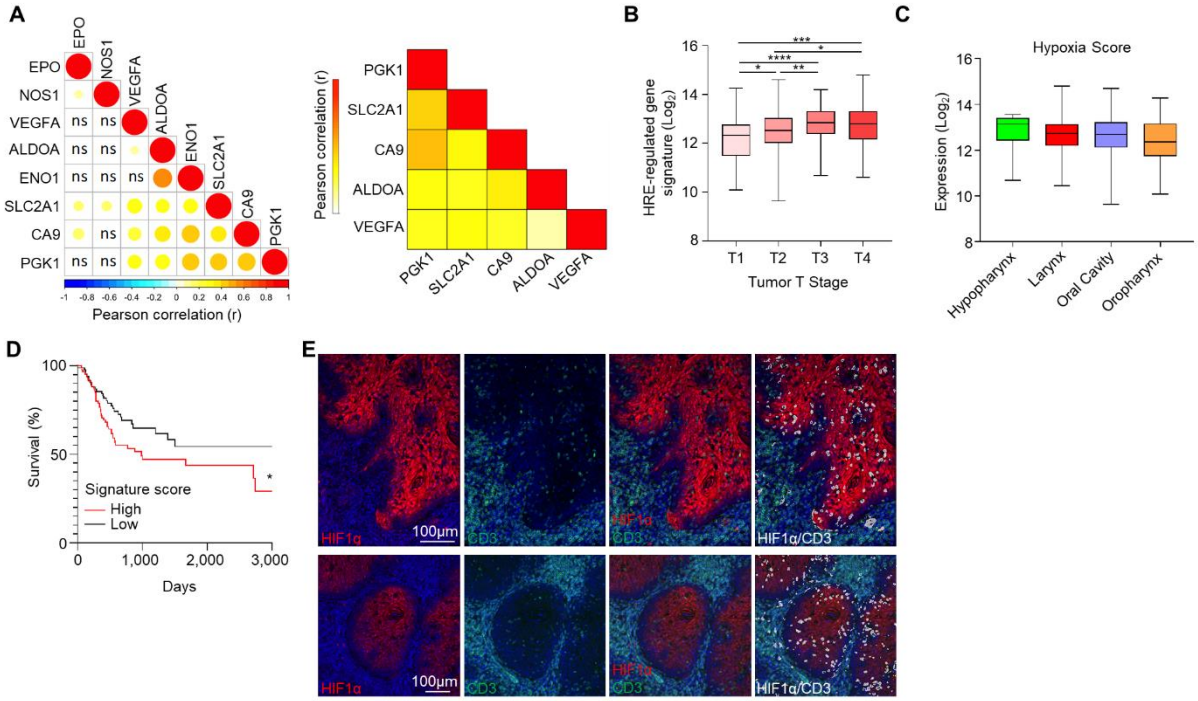

Figure S5. HRE-regulated gene signature and HIF1α in HNSCCs to identify patient cohorts more likely to benefit from HypoxiCAR immunotherapy. Related to Figure 4. **(A-D)** An HRE-regulated gene signature was constructed from known HRE-regulated genes in the HNSCC TCGA dataset (n=528). (**A**) Correlation plot showing pairwise correlation of HRE-regulated genes in the HNSCC. The size of the dot represents the *P* value of the correlation where $P > 0.05$ and the color of the dot represents the Pearson correlation coefficient (r) (left) and heatmap displaying the Pearson correlation coefficient for the individual genes in the TCGA HNSCC dataset (right). (**B**) Signature expression based on T stage (T1 n=48, T2 n=136, T3 n=99, T4 n=174). (**C**) Expression of the HRE-regulated gene score in HNSCC based on subtype (hypopharynx n = 10, larynx n = 116, oral cavity n = 316, oropharynx n = 79). (**D**) Survival curve for patients with Stage 3 and 4 HNSCC for high and low expression of the HRE-regulated gene signature (n=87 respectively). (**E**) Additional representative confocal images from sections from two further HNSCC tumors stained with DAPI (nuclei; blue) and antibodies against CD3 (green) and HIF1α (red), white events denote CD3 and HIF1α co-localizing pixels. Images are representative of multiple tissues and sections. Box plots show median and upper/lower quartiles, whiskers show highest and lowest value. Bar chart shows the group mean and each dot represents an individual mouse and tumor. * $P<0.05$,** $P<0.01$, *** $P<0.001$, **** $P<0.0001$.